Available online at www.sciencedirect.com
SCIENCE DIRECT
Physica C 443 (2006) 9–17
PHYSICA C
www.elsevier.com/locate/physc

Physical properties of $YBa_2Cu_3O_{7-\delta}$ thin films using microstrip ring resonators technique

L.S. Lai [a,*], H.K. Zeng [b], J.Y. Juang [a], K.H. Wu [a], T.M. Uen [a], J.Y. Lin [c], Y.S. Gou [a]

[a] Department of Electrophysics, National Chiao-Tung University, Hsinchu 30050, Taiwan
[b] Department of Electronic Engineering, Chung-Yuan Christian University, 200 Chung-Pei Road, Chung-Li 32023, Taiwan
[c] Institute of Physics, National Chiao-Tung University, Hsinchu 30050, Taiwan

Received 3 November 2005; received in revised form 11 April 2006; accepted 21 April 2006

Abstract

Microstrip ring resonators with quality factor (Q) over 10^4 at temperature 5 K, were fabricated using the double-side $YBa_2Cu_3O_{7-\delta}$ (YBCO) epitaxial films deposited on $LaAlO_3$ (LAO) substrates. By placing a narrow gap in the ring resonator, we observed that the original fundamental resonating mode (resonance frequency $f = 3.61$ GHz) splits into a dual-mode with different resonating frequencies ($f = 1.80$ GHz and $f = 5.33$ GHz). These two kinds of the resonator allow us to determine the temperature and frequency dependences of the magnetic penetration depth $\lambda(T,f)$ and the surface loss. Several salient features of the above findings related to the nature of low-lying excitations for high-T_c superconductivity as a function of oxygen content will be elucidated. In particular, the current models, suggested by Wen and Lee, will be examined in a quantitative manner. It allows us to give a justification of quasiparticle as Fermi-liquid in the superconducting state. In addition, an equivalent inductance circuit model is suggested to account for the occurrence of the dual-mode resonance.

PACS: 74.72.Bk; 74.25.Nf; 74.78.Bz

Keywords: Microwave ring resonators; Dual-mode resonance; Magnetic penetration depth

1. Introduction

Microwave ring resonators made of an annular ring with high-T_c superconducting (HTS) thin films, combined with the same superconducting ground plane, are of considerable theoretical and practical interests owing to their geometry advantages in greatly resolving the extremely non-uniform current distribution and reducing inductance commonly encountered by the stripline resonators [1–7]. Such resonator always manifests itself with a degenerate fundamental mode. If one put forth a gap structure in the microstrip ring resonator, it is then expected to split into a dual-mode resonator. The frequencies of the dual-mode are dependent upon the location of the gap with respect to the coupling lines [3]. Such microwave technique provides advantage over the previous one in the measurements of the frequency dependences of the penetration depth and its derived and related physical quantity with a unique sample.

Firstly, in an attempt to clarifying the origin of the dual-mode resonance, we manipulated the geometrical configuration of the sample by introducing a split gap, which is symmetrical with respect to the coupling lines, into our YBCO ring resonator structure, as shown in Fig. 1. With the insight on the microwave properties of the resonator with and without the gap, a consistent physical property of generating the dual-mode in a unique sample can be elucidated in the light of an equivalent inductance-circuit

* Corresponding author. Tel.: +886 3 5712121 56111; fax: +886 3 572 5230.
E-mail address: u9021807@cc.nctu.edu.tw (L.S. Lai).

0921-4534/$ - see front matter © 2006 Published by Elsevier B.V.
doi:10.1016/j.physc.2006.04.089

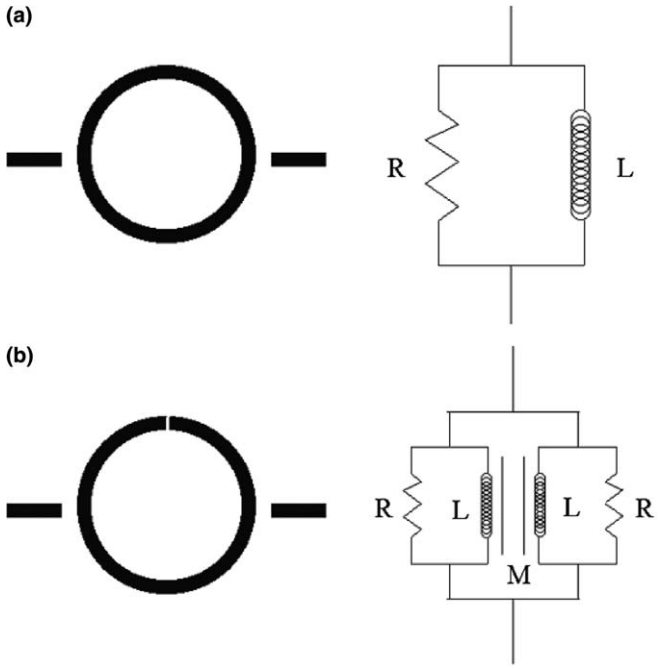

Fig. 1. An equivalent circuit of the ring shaped microstrip resonator (a) without or (b) with a split gap.

model. Using such kinds of samples with a proper control of various oxygen contents [4], a number of unique features of low-lying excitations (quasiparticles) of the high-T_c underdoped cuprates in the superconducting state can be explored detail.

In this report, the temperature and frequency dependences of the penetration depth $\lambda(T,f)$ and the surface loss will be extracted from the measurements of the surface impedance and the quality factor of the resonator together with the proper geometrical factor, respectively. As compared to the previous works, we believe that all these findings not only allow us to give some reliable evidences related to the nature of the superconducting carrier density, but also provide a great amount of viable data to shed light on the model construction of the superconductivity mechanism under the strong impurity scattering.

2. Experiment and data analysis

The YBCO thin films used for fabricating the ring resonators were deposited epitaxially on both sides of a 0.5 mm thick $LaAlO_3$ substrate by pulsed laser deposition [8]. The substrate temperature was kept at 830 °C, and the oxygen partial pressure was maintained at 280 mTorr during the deposition. Both films were c-axis oriented, with thickness of 500 nm and $T_c = 90$ K. One side of the films was then patterned into the ring shaped microstrip line with or without a split gap, as shown schematically in Fig. 1. The line width, split gap and the outer radius of the ring are 0.5 mm, 0.1 mm and 3.625 mm ($\approx r_o$), respectively. The coupling gap between the microstrip feeding line and the ring resonator is about 0.4 mm. The main difficulty for double side deposition is the contact between the substrate and the heater, which has been solved by inserting a thin Si-wafer between the substrate and the heater. This effectively prevents the backside of the polished substrates as well as the first film during the deposition of the second one from contamination. The fact provides a great advantage to give a rather simple treatment in theoretical consideration to derive the penetration depth.

To obtain the desired oxygen content of the YBCO films, the sample was put in a YBCO bulk housing and the whole assembly was situated in an oxygen annealing chamber. The oxygen pressure and the corresponding temperature were then carefully monitored following the pressure-temperature phase diagram established for YBCO system [9]. This process had been confirmed to be capable of obtaining designated oxygen content of YBCO films in a controllable and reversible manner [10].

The microstrip ring resonator was put into an Au-coated aluminum housing with SMA connectors. The package was placed in a vacuum tube and immersed in liquid He. We used a Lake Shore 330 autotune temperature controller to control the temperature of the sample space to better than 0.1 K. The temperature dependence of the resonance frequency $f(T)$, the resonator bandwidth at -3 dB, $\delta f(T)$, and the forward transmission coefficient S_{21} were measured by a HP8510C microwave vector network analyzer.

The loaded quality factor Q_L of the resonator was derived from the full bandwidth δf at half maximum (FWHM) of the transmission curve $S_{21}(f)$ using $Q_L = f_0/\delta f$, where f_0 is the resonance frequency. Unloaded quality factor Q_u is calculated using $Q_u = Q_L/(1 - S_{21})$. The dielectric loss of the $LaAlO_3$ substrates is lower than 5×10^{-6} at temperature below T_c of the YBCO, and it was neglected in our case. Since the losses due to radiation have been minimized by providing effective shielding at half wavelength spacing around the device, they can be neglected as compared to the dielectric loss. Thus the Q_u comes mainly from the surface resistance R_s of the superconducting ring and the ground plate. From the unloaded quality factor Q_u and the resonance frequency $f(T)$, the surface resistance R_s and reactance X_s consisting of surface impedance $Z_s(T) = R_s(T) + iX_s(T)$ are calculated with the aid of the formula [11]:

$$R_s(T) = \Gamma/Q_u(T), \tag{1}$$

$$X_s(T) - X_s(T_0) = -2\Gamma[f(T) - f(T_0)]/f(T), \tag{2}$$

where Γ is the geometry factor of the resonator and T_0 is the lowest temperature in the experiment ($T_0 = 5$ K). Actually, Γ depends [11–13] on the penetration depth λ and geometry parameters (such as the microstrip width W, substrate thickness h, thin film thickness t) of the superconducting resonator if t/λ is not much larger than 1. The value of Γ can be calculated by the method of incremental frequency rules [14–16] via

$$\Gamma = \mu_0\omega^2/4\{-\Delta\omega/\Delta\lambda\}^{-1}, \quad (3)$$

where $\Delta\omega/\Delta\lambda$ is the derivative of the angular resonance frequency ($\omega = 2\pi f$) with respect to the penetration depth $\lambda(T)$. Using Chang's formula [17] for the inductance and capacitance of a superconducting strip line the angular resonance frequency is given by

$$\omega(T) = (c/\varepsilon^{1/2}L)\{1 + \lambda(T)/d[2\coth(t/\lambda(T)) + g\mathrm{csch}(t/\lambda(T))]\}^{-1/2}, \quad (4)$$

where ε is the dielectric constant of the substrate, d is the effective substrate thickness, L is the length of the strip line, g is a fringe factor, and c is the velocity of the light in vacuum. By inserting $\Delta\omega/\Delta\lambda$ obtained from Eq. (4) into Eq. (3), Γ can be derived as

$$\Gamma = (1/2)\mu_0\omega d\{1 + \lambda/d[2\coth(t/\lambda) + g/\sinh(t/\lambda)]\}/\{\coth(t/\lambda) + (t/\lambda)/\sinh^2(t/\lambda) + g[1 + (t/\lambda)\coth(t/\lambda)]/[2\sinh(t/\lambda)]\}, \quad (5)$$

where g is a correction factor accounting for the fringe field effect as the aspect ratio W/d of the stripline near or less than 1. On the other hand, we have the relation between the surface reactance $X_s(T)$ and the penetration depth $\lambda(T)$ [16,18], i.e., $X_s(T) = \mu_0\omega\lambda(T)$. Thus, from Eq. (2), one obtains

$$\mu_0\omega[\lambda(T) - \lambda(T_0)] = 2\Gamma[f(T_0) - f(T)]/f(T). \quad (6)$$

When $t/\lambda(T) \gg 1$, the formula (5) can be simplified to:

$$\Gamma = (1/2)\mu_0\omega d. \quad (7)$$

In this case we can get $\Delta\lambda$ from $f(T)$ curve directly. In general case $t/\lambda(T) \gg 1$ is not fulfilled instead, we have to fit the curve, $f(T)$, to give the penetration depth. It is convenient to use the normalized form of Eq. (4):

$$\frac{f(T)}{f(T_0)} = \frac{\sqrt{1 + \frac{\lambda(T_0)}{d}\left\{2\coth\left(\frac{t}{\lambda(T_0)}\right) + g\mathrm{csch}\left(\frac{t}{\lambda(T_0)}\right)\right\}}}{\sqrt{1 + \frac{\lambda(T)}{d}\left\{2\coth\left(\frac{t}{\lambda(T)}\right) + g\mathrm{csch}\left(\frac{t}{\lambda(T)}\right)\right\}}}. \quad (8)$$

Here T_0 is the lowest temperature in the experiments, which is around 5 K in our case. To obtain the absolute values of $\lambda(T)$, the modified two-fluid model has to be assumed. Following a number of previous studies we will take:

$$\lambda(T) = \lambda(5\ \mathrm{K})\left[1 - \left(\frac{T}{T_c}\right)^2\right]^{-\frac{1}{2}}, \quad (9)$$

at $0.3 \leqslant T/T_c \leqslant 0.6$. Using (8) and (9), then the best fit to the experimental curves $f(T)$ gets the $\lambda(5\ \mathrm{K})$. For example, the best least-square fit yields $d = h/4$ and $\lambda(5\ \mathrm{K}) = 150$ nm for $\delta = 0.05$, as shown in Fig. 2(a)–(c) at frequencies 1.80 GHz, 3.61 GHz, and 5.33 GHz respectively. The obtained value of $\lambda(5\ \mathrm{K})$ was then inserted into Eq. (8) to obtain $\lambda(T)$ for all temperatures. The results for films with various oxygen contents are listed in Table 1. It is noted that, for $\delta = 0.05$ (i.e. the optimal doped YBCO), the value of $\lambda(5\ \mathrm{K}) = 150$ nm is very close to that reported for single crystalline YBCO [19,20] and $d = h/4$ is also consistent with the justification of the geometrical structure of the microwave ring resonator as compared with the strip line.

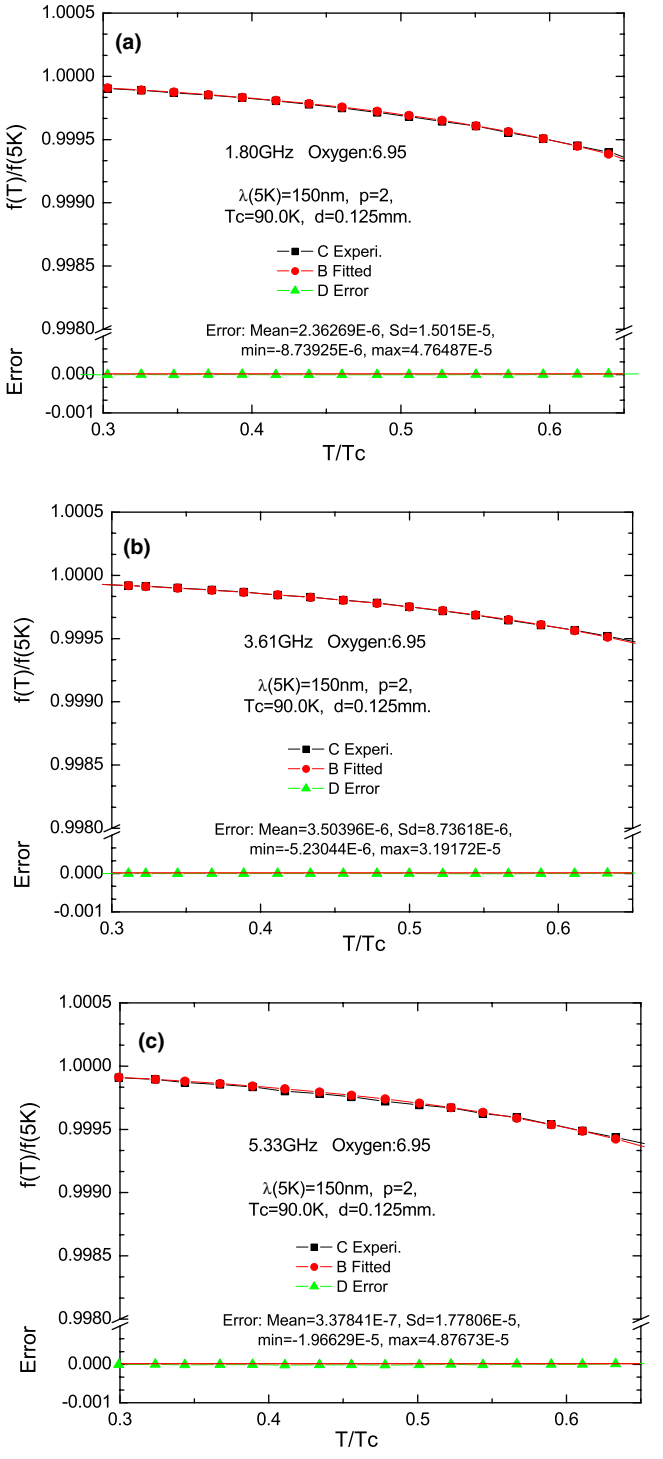

Fig. 2. The fitting to the normalized temperature dependence of $f(T)/f(5\ \mathrm{K})$ at resonance frequencies: (a) $f = 1.80$ GHz, (b) $f = 3.61$ GHz and (c) $f = 5.33$ GHz in the temperature range $0.3 \leqslant T/T_c \leqslant 0.6$ for oxygen content $\delta = 0.05$.

Table 1
Some parameters for $YBa_2Cu_3O_{7-\delta}$ thin films are obtained from microwave ring resonators [30]

$7-\delta$	f (GHz)	λ(5 K) nm	$2\Delta(0)/T_c$	d[λ^2(5 K)/$\lambda^2(T)$]/dT (K^{-1})	v_F/v_Δ	α^2
6.95	3.61	150 ± 14	6.1 ± 2.2	$1/(250 \pm 50)$	14	0.43 ± 0.17
	1.80		6.8 ± 0.9	$1/(212 \pm 29)$		0.52 ± 0.18
	5.33		7.2 ± 1.0	$1/(370 \pm 100)$		0.34 ± 0.16
6.8	3.61	216 ± 16	6.0 ± 0.5	$1/(200 \pm 26)$	10.1	0.35 ± 0.08
	1.80		6.5 ± 0.5	$1/(189 \pm 29)$		0.38 ± 0.09
	5.33		6.4 ± 0.7	$1/(197 \pm 17)$		0.37 ± 0.07
6.6	3.61	282 ± 20	5.0 ± 0.6	$1/(91 \pm 10)$	8.7	0.53 ± 0.08
	1.80		5.9 ± 1.1	$1/(119 \pm 13)$		0.41 ± 0.06
	5.33		6.6 ± 0.6	$1/(127 \pm 10)$		0.39 ± 0.05

3. Results and discussion

We briefly review the effect of a split gap on a microstrip ring resonator. When the split gap is located at the symmetrical position of the ring with respect to the coupling lines, the original resonance frequency at 3.61 GHz evidently split into the dual stationary modes at 1.80 GHz and 5.33 GHz, respectively. This result has been studied previously [3]. To understand the origin of this effect, an equivalent circuit model has been put forth to describe the stationary behavior of this dual-mode resonance. Since the magnetic field is the dominant relevant parameter inside the superconducting microstrip ring resonator, we will take only the inductive effect into account. By coupling through the input port, the microwave currents flowing inside the microstrip ring resonator can be, to the first approximation, written as

$$\begin{aligned} L_{11}\frac{dI_1}{dt} &= i\omega_0 L_{11} I_1 + i\omega_0 L_{12} I_2, \\ L_{22}\frac{dI_2}{dt} &= i\omega_0 L_{21} I_1 + i\omega_0 L_{22} I_2, \end{aligned} \tag{10}$$

where I_1 and I_2 are the amplitudes of the current density wave flowing clockwise and counterclockwise, respectively. L_{11} and L_{22} are self-inductance coefficient ($L_{11} = L_{22}$ in our case). L_{12} and L_{21} are mutual inductance coefficient ($L_{12} = L_{21}$, for the symmetrical configuration). The system essentially manifests itself as a simple two-state system and any structure perturbation in the perfect ring does may provide a coupling between the two degenerate states. When there is no coupling, as in the case of the perfect ring resonator, the equations become

$$\begin{aligned} L_{11}\frac{dI_1}{dt} &= i\omega_0 L_{11} I_1, \\ L_{22}\frac{dI_2}{dt} &= i\omega_0 L_{22} I_2. \end{aligned} \tag{11}$$

Since $L_{11} = L_{22}$ in our case, one obtains in the stationary case

$$\begin{aligned} I_1 &= A e^{i\omega_0 t}, \\ I_2 &= B e^{i\omega_0 t}, \end{aligned} \tag{12}$$

with A and B being constants. The solutions indicate the inherent resonance degeneracy of the structure. Eq. (10) though does not specify how coupling between the degenerate resonant mode can be introduced, it has been demonstrated experimentally that various kinds of the structure perturbation along the periphery of the ring may result in a splitting in the resonance frequencies [7]. In our case, the introduction of a "split-gap", which is symmetrical with respect to the coupling lines, turns out to give rise to an even more pronounced splitting effect. It is conceived that the electromagnetic waves totally reflected at the gap barrier may act as the cause of the mutual inductance. By taking $L_{12} = L_{21} = -M$, the mutual inductance depending only on the circuit geometry, Eq. (10) can be rewritten as

$$\begin{aligned} L_{11}\frac{dI_1}{dt} &= i\omega_0 L_{11} I_1 - i\omega_0 M I_2, \\ L_{22}\frac{dI_2}{dt} &= i\omega_0 L_{22} I_2 - i\omega_0 M I_1. \end{aligned} \tag{13}$$

The solutions to Eq. (13) are

$$\begin{aligned} I_1 &= \frac{C}{2} e^{i\left(\omega_0 - \omega_0 \frac{M}{L_{11}}\right)t} + \frac{D}{2} e^{i\left(\omega_0 + \omega_0 \frac{M}{L_{11}}\right)t}, \\ I_2 &= \frac{C}{2} e^{i\left(\omega_0 - \omega_0 \frac{M}{L_{22}}\right)t} - \frac{D}{2} e^{i\left(\omega_0 + \omega_0 \frac{M}{L_{22}}\right)t}, \end{aligned} \tag{14}$$

where C and D are constants. When either C or D is zero, the system is in stationary resonant mode. Namely, when $D = 0$, I_1 and I_2 are in phase (since $L_{11} = L_{22}$ in our case), and the system is at a stationary state with a definite frequency $\omega_0 - \omega_0 M/L_{11}$. On the other hand, when $C = 0$, I_1 and I_2 are out of phase with another definite frequency of $\omega_0 + \omega_0 M/L_{11}$. Physically, the scenario is very similar to other simple two-state systems with coupling, for example, a coupled two-pendulum problem. In any two-state system the strength of the coupling is, in general, originated from some perturbations in the system. Thus it is also very convenient to obtain the coupling strength from the measurements of the resonance frequencies with the aid of the above the circuit model. In our case, the split of the degenerate resonance frequency (ω_0) to $\omega_0/2$ and $3\omega_0/2$ implies an inductance ratio $M/L_{11} = 1/2$. This result can be easily justified by the measured resonance frequencies of the ring resonators with and without a split gap.

In order to further confirm the above assertion of regarding the ring resonator as a simple two-state system as well as the split gap induced mutual inductance scenario, numerical simulations using electromagnetic simulator Ensemble of "ANSOFT" corporation to depict the current density wave distributions along the ring were performed. Resonance frequencies and the corresponding standing wave pattern obtained by assuming a perfect conductor ring with the same physical and geometric parameters of the real resonator are depicted in Fig. 3(a). Fig. 3(a) shows the fundamental degenerate modes manifested in the full ring structure. The two current density nodes on the opposite sides of the ring resonator with a resonating

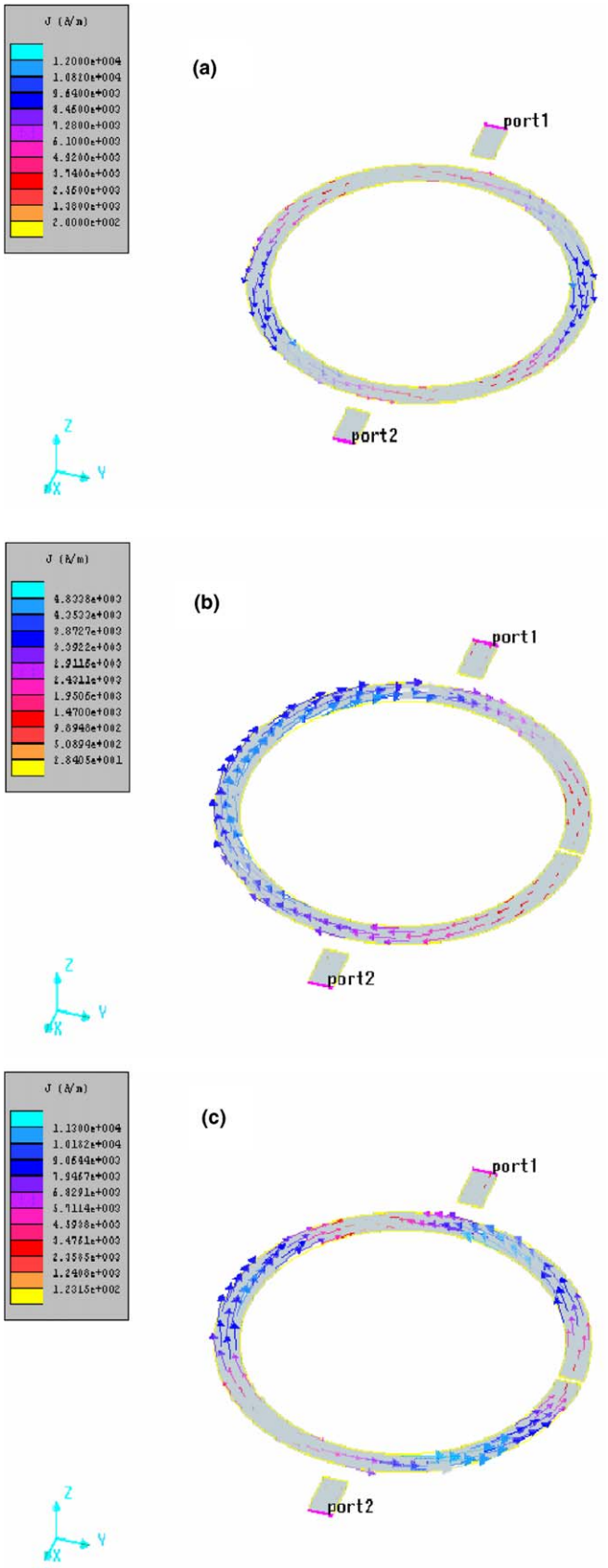

Fig. 3. (a) The fundamental degenerate modes ($\lambda_p = 2\pi r_o$) manifested in the perfect ring structure. For rings with a split gap at half-way between the two coupling ports, one obtains two fundamental modes with the resonant frequencies of (b) $\lambda_p/2 = 2\pi r_o$ and (c) $3\lambda_p/2 = 2\pi r_o$, respectively.

wavelength $\lambda_p = 2\pi r_o$ are evident. For rings with a split gap at half-way between the two coupling ports, one obtains two fundamental modes with the resonant frequencies of $\lambda_p/2 = 2\pi r_o$ (Fig. 3(b)) and $3\lambda_p/2 = 2\pi r_o$ (Fig. 3(c)), respectively. In both cases the position of the split gap always coincides with the node of current density waves. In any case, we note that in either mode the phase velocity of the current density wave remains unchanged, indicative of the nondispersive nature of superconductors.

Fig. 4(a) and (b) show the systematic changes of the $|S_{21}|$ obtained at 5 K for both resonance frequencies (1.80 GHz and 5.33 GHz) when the oxygen content of the same YBCO ring resonator with a split gap was varied intentionally from $\delta = 0.05$ to $\delta = 0.4$. The removal of oxygen in YBCO is known to take place primarily at the Cu–O chain, leading to a reduction of superfluid density and longer London penetration depths (λ_L). As a result, the shifts to lower resonance frequencies observed in both modes with decreasing oxygen content are due primarily to the increasing λ_L. The other peculiar feature to be noted is the magnitude of $|S_{21}|$ appears to decrease with decreasing oxygen in YBCO for the lower frequency mode, while the opposite trend is evident for the higher frequency mode. The fact how reducing oxygen would enhance $|S_{21}|$ of one mode while suppress the other is not clarified yet.

In Fig. 5, the temperature dependence of the unloaded quality factor, Q_u for fully oxygenated YBCO ring resonator displays essentially the same behavior for the cases of the frequencies at 1.80 GHz and 3.61 GHz regardless of

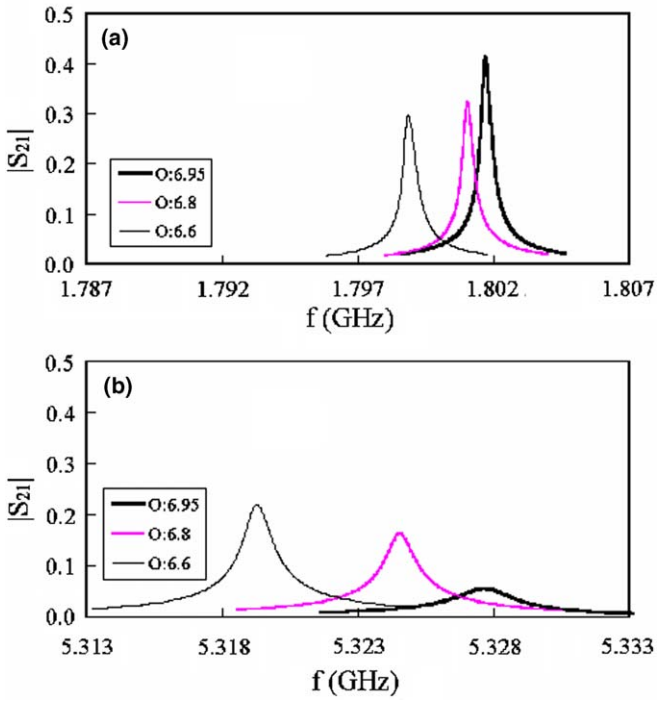

Fig. 4. (a) The frequency dependence of the forward transmission coefficient $|S_{21}|$ of the split gap resonator obtained at 5 K on the one mode ($f = 1.80$ GHz) for $\delta = 0.05$, 0.2 and 0.4, respectively. The result of another mode ($f = 5.33$ GHz) is shown in (b).

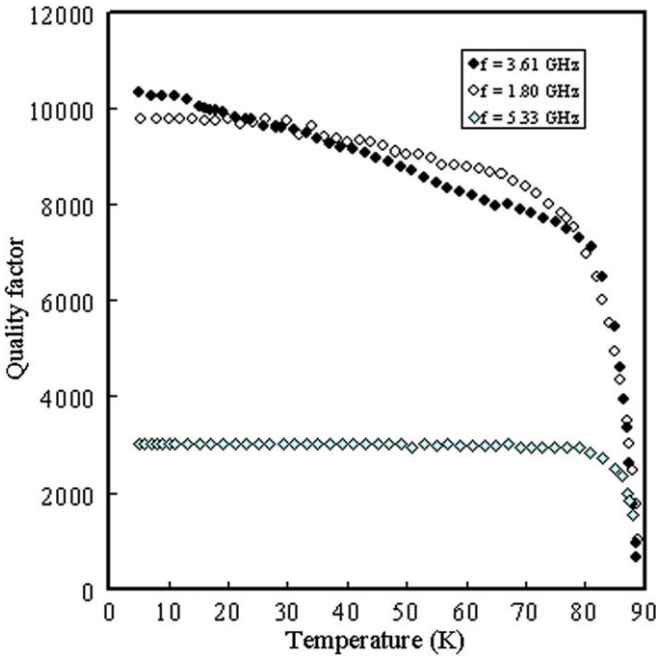

Fig. 5. The temperature dependence of the quality factor for the ring resonators with and without a split gap.

the existence of the split gap. This implies that Q_u is not affected even when the geometrical symmetry of the ring resonator is broken. Moreover, from the measurement of Q_u and the calculation of the geometrical factor Γ, we can obtain the surface resistance R_s, as shown in Fig. 6. Fig. 6 also shows that the ratio of R_s values for 3.61 and 1.80 GHz is about 4, while the ratio between 5.33 and 1.80 GHz rises by a factor of 9. This is consistent with the fact that R_s should be proportional to ω^2 in the London limit. Herein the values of penetration depth λ are independent of frequencies.

We would like to turn the attention to examine some fundamental property of $\lambda(T)$ using the present resonating structures. This is one of the most intriguing issues on high-T_c superconductivities. In particular, the temperature dependence and the slope of the dependence are the important relevant parameters revealing of the order-parameter symmetry as well as providing rich information about the nature of low-lying excitations. As shown in Figs. 7 and 8, $\Delta\lambda(T)$ as a function of oxygen content derived from the low frequency mode (1.80 GHz) in the split YBCO ring resonator and 3.61 GHz in the perfect one, respectively, display the same linear-temperature dependent features. However, the linear-temperature dependent range of $\Delta\lambda(T)$ is different for the two resonance frequencies. For $\delta = 0.05$, $\Delta\lambda(T)$ displays a linear behavior up to temperature $T = 35$ K for the perfect ring resonator, as shown in Fig. 8. But for the ring resonator with a split gap, $\Delta\lambda(T)$ displays a linear behavior at $T < 25$ K for $\delta = 0.05$. Furthermore, for $\delta = 0.2$ and 0.4 [21], similar peculiarities are observed, except that the respective corresponding temperatures are lower. All the above-mentioned features of the resonator with a split gap at 5.33 GHz were similar to those at 1.80 GHz but were different comparing with the perfect ring resonator. The effect of introducing a geometrical gap in suppressing the temperature dependence of

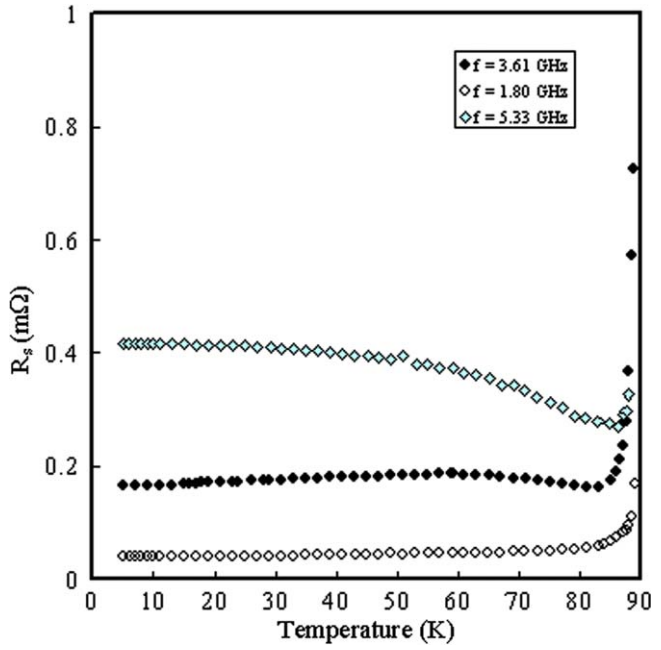

Fig. 6. The temperature dependence of surface resistance R_s ($\delta = 0.05$) of the YBCO ring resonator with and without a split gap measured for $f = 1.80$, 3.61, and 5.33 GHz, respectively.

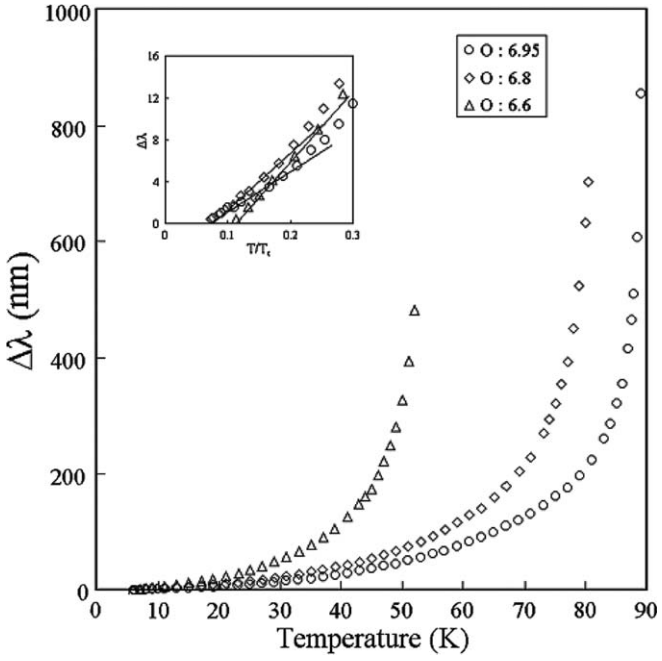

Fig. 7. The temperature dependence of the $\Delta\lambda(T)$ as a function of oxygen content derived from the low frequency mode (1.80 GHz) in split gap ring resonator. The inset shows the normalized temperature dependence of the $\Delta\lambda(T)$ for $\delta = 0.05$, 0.2 and 0.4, respectively.

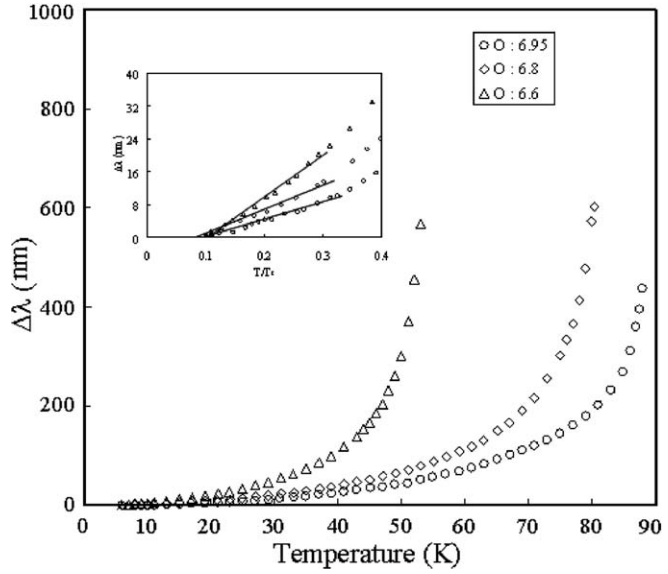

Fig. 8. The temperature dependence of the $\Delta\lambda(T)$ as a function of oxygen content in the perfect ring resonator. The inset shows the normalized temperature dependence of the $\Delta\lambda(T)$ for $\delta = 0.05$, 0.2 and 0.4, respectively.

$\Delta\lambda(T)$ in the low temperature regime was observed here, and this effect was very similar to the study done by Bonn et al. [22] who observed that the properties of $\Delta\lambda(T)$ were very sensitive to defects. The interesting problem is, however, not clarify yet.

At the low temperature regime ($T < T_c/3$), moreover, we can estimate the ratio of the maximum energy gap $\Delta(0)$ and the critical temperature T_c, from Scalapino's [23] theoretical formula, $\Delta\lambda/T = \lambda(0)\ln 2/\Delta(0)$ for the d-wave pairing, where we assume $\lambda(0) \approx \lambda(5\,\mathrm{K})$. The value of $2\Delta(0)/T_c$ is approximated to a constant value ($\approx 6.0 \pm 0.6$), which is independent of oxygen concentrations. The value of $\lambda(5\,\mathrm{K})$ depends on the hole concentration greatly. And all $\lambda(5\,\mathrm{K})$ are independent of the frequency. Finally, $\lambda(T)$ behaves as a universal manner in terms of the normalized temperatures, (T/T_c). The fact is thus strongly evident that a unique nature of the high-T_c superconducting mechanism is shown in the CuO_2 plane.

Fig. 9 shows the normalized temperature dependence of the $\lambda^2(5\mathrm{K})/\lambda^2(T)$ at 1.80 GHz, which denotes the change of the superfluid density by decreasing temperature. It is clearly evident that it is almost independent of the doping concentrations in terms of the normalized temperature ($T/T_c < 0.3$). In the low temperature regime, the linear T dependence is also observed, as shown in Fig. 10, while the slope increases as δ increasing. The independent property of the doping concentration reflects a fact that the Cu–O chain in the YBCO material is not a crucial factor in the consideration of superconductor properties. In fact the linear temperature dependence will provide a valuable data to estimate the Fermi-liquid correction factor, α^2, together with the measurement of the thermal conductivity. It allows us to test the theoretical model suggested by Lee and Wen [24,25] in a quantitative way. The slope of normalized superfluid density $\lambda^2(0)/\lambda^2(T)$, following their model, is related to the Fermi-liquid correction factor, α^2, and the thermal conductivity [26], κ_0/T, as

$$\frac{d\lambda^{-2}(T)}{dT} = -2.93 \times 10^{13}\frac{\kappa_0}{T}\alpha^2. \quad (15)$$

For the optimally doped sample, the κ_0/T value of $0.14\,\mathrm{mW/K^2\,cm}$ can be taken from the thermal conductivity measurements of YBCO single crystal [26] for the thin films. Hence the Fermi-liquid correction factor α^2 could be calculated as

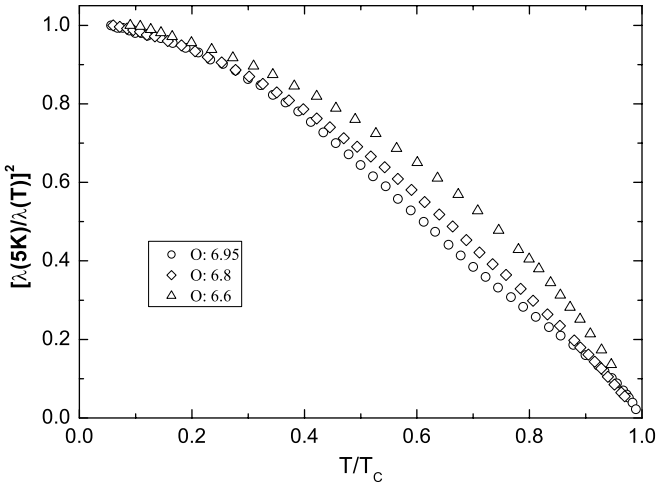

Fig. 9. The $\lambda^2(5\,\mathrm{K})/\lambda^2(T)$ vs. reduced temperature T/T_c for the low frequency mode (1.80 GHz) in split gap ring resonator with various oxygen contents.

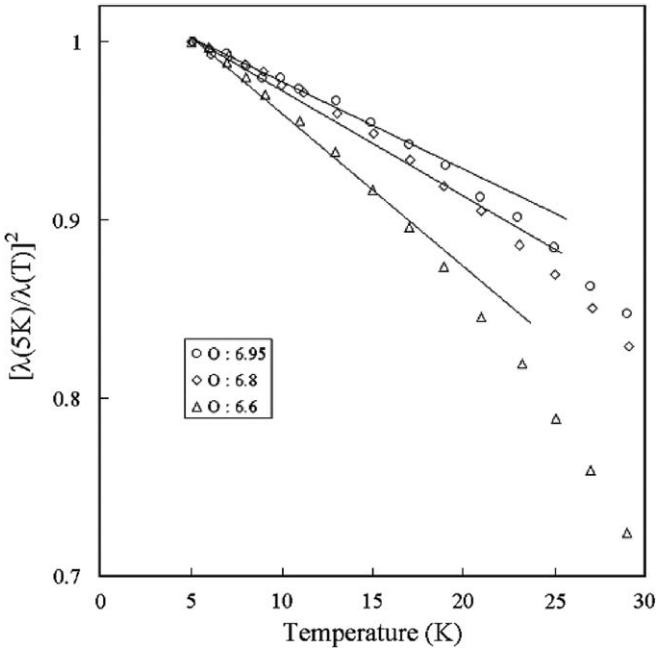

Fig. 10. The $\lambda^2(5\,\mathrm{K})/\lambda^2(T)$ vs. temperature T in the lower temperature region for the low frequency mode (1.80 GHz) in split gap ring resonator with various oxygen contents.

$$\alpha^2 = -\frac{2.44\times10^{-12}}{\lambda^2(5\text{ K})}\frac{\mathrm{d}[\lambda^2(5\text{ K})/\lambda^2(T)]}{\mathrm{d}T}. \quad (16)$$

For the underdoped samples, more elaborate consideration is necessary to elucidate the accurate value of α^2. In the cuprates, $\kappa_0/T \approx (k_B^2/3\hbar)(n/d)(v_F/v_\Delta)$ where n/d is the stacking density of CuO_2 planes, v_F is the Fermi velocity, and v_Δ is the energy dispersion along the Fermi surface at nodes [27,28]. Assuming the tendency of v_F/v_Δ with respect to p of single crystal data in Ref. [29] is qualitatively and quantitatively applicable to our samples, the values of α^2 for various oxygen contents are now accessible. The values of α^2 for various oxygen contents [30] and some other important findings are listed as follows and in Table 1. It is found that in these oxygen contents ($\delta = 0.05$–0.4) studied in this paper, α^2 is less than 1. Therefore, the Fermi liquid corrections for quasiparticles in the underdoped cuprates are not negligible. The values of α^2 are between 0.4 and 0.6, and are almost identical to that in Ref. [29]. At last, the values of α^2 for the cuprate samples studied in this work are nearly independent of frequencies.

4. Summary

Microstrip ring resonators made of double-side YBCO films have been demonstrated to have great potential for science and engineering applications. From the frequency dependence of the forward transmission coefficient $|S_{21}|$, it was found that the resonating frequency split into a dual-mode by introducing a geometric gap. The equivalent mutual-inductance-circuit model was proposed to delineate the occurrence of the dual stationary modes. Taking advantage of the characteristic features of the device, some intriguing results of the temperature and frequency dependences of the physical properties were obtained in the samples with various oxygen contents. Some salient results are listed below:

1. For fully oxygenated case ($\delta = 0.05$), the resonator exhibits a quality factor $Q > 10^4$ around 15 K, and $\Delta\lambda(T) = \lambda(T) - \lambda(5\text{ K})$ displays a linear behavior at $T < 35$ K for the perfect ring resonator ($f = 3.61$ GHz). But for the ring resonator with a split gap ($f = 1.80$ GHz and $f = 5.33$ GHz), the linear-T dependent range of $\Delta\lambda(T)$ becomes smaller ($T < 25$ K). With increasing δ (e.g. $\delta = 0.2$, 0.4), although $\Delta\lambda$ is still linear in temperature, the slope changes with increasing oxygen deficiency.
2. Following the model suggested by Scalapino, the energy gap could be derived and the value of the ratio of energy gap to the critical temperature, we found $2\Delta(0)/k_BT_c$, around 6.0 ± 0.6, which is independent of the doping concentrations.
3. The function of $\lambda(T)$ versus the normalized temperature T/T_c exhibits a universal form. It implies a unique high-T_c mechanism in the underdoped cuprate, which is occurred in the CuO_2 planes only. This fact is consistent with the observations of μSR data by Tallon et al. [19]. The values of $\lambda(5\text{ K})$ with various oxygen contents are 150 ± 14 ($\delta = 0.05$), 216 ± 16 ($\delta = 0.2$) and 282 ± 20 nm ($\delta = 0.4$), respectively and found to be independent of frequencies.
4. The Fermi-liquid correction factor α^2 predicted by Lee and Wen's model can be obtained with the values between 0.4 and 0.6 from the optimum ($\delta = 0.05$) to the underdoped ($\delta = 0.4$) cuprates. The result gives a justification of the quasiparticle as Fermi-liquid in the superconducting state.

Acknowledgement

This work was supported by the National Science Council of Taiwan, ROC under grant: NSC 89-2112-M-009-028.

References

[1] H.K. Zeng, J.Y. Juang, J.Y. Lin, K.H. Wu, T.M. Uen, Y.S. Gou, Physica C 351 (2001) 97;
H.K. Zeng, J.Y. Juang, K.H. Wu, T.M. Uen, Y.S. Gou, Physica C 341–348 (2000) 2669.
[2] H.Y. To, G.J. Valco, K.B. Bhasin, Supercond. Sci. Technol. 5 (1992) 421.
[3] H.K. Zeng, Y.S. Gou, J.Y. Juang, K.H. Wu, T.M. Uen, Physica C 341–348 (2000) 2665.
[4] L.S. Lai, J.Y. Juang, K.H. Wu, T.M. Uen, J.Y. Lin, Y.S. Gou, Physica C 415 (2004) 133.
[5] C.M. Chorey, K.S. Kong, K.B. Bhasin, J.D. Warner, T. Itoh, IEEE Trans. Microwave Theory Technol. MTT-39 (1991) 1480.
[6] S.Y. Lee, K.Y. Kang, D. Ahn, IEEE Trans. Appl. Supercond. 5 (1995) 2563.
[7] I. Wolfe, Electron. Lett. 8 (1972) 302.
[8] M.C. Hsieh, T.Y. Tseng, S.M. Wei, C.M. Fu, K.H. Wu, J.Y. Juang, T.M. Uen, Y.S. Gou, Chin. J. Phys. 34 (1996) 606.
[9] P.K. Gallagher, Adv. Ceram. Mater. 2 (1987) 632.
[10] K.H. Wu, M.C. Hsieh, S.P. Chen, S.C. Chao, J.Y. Juang, T.M. Uen, Y.S. Gou, T.Y. Tseng, C.M. Fu, J.M. Chen, R.G. Liu, Jpn. J. Appl. Phys. 37 (1998) 4346.
[11] M.J. Lancaster, Passive Microwave Devices Applications of High-Temperature Superconductors, Cambridge University Press, 1997.
[12] D.E. Oates, A.C. Anderson, D.M. Sheen, S.M. Ali, IEEE Trans. Microwave. Theory. Technol. MTT-39 (1991) 1522.
[13] A. Porch, M.J. Lancaster, R. Humphreys, IEEE Trans. Microwave Theory Technol. MTT-43 (2) (1995) 306.
[14] D.E. Oates, A.C. Anderson, IEEE Trans. Magn. MAG-27 (1991) 867.
[15] D. Kajfez, IEEE Trans. Microwave. Theory. Technol. MTT-32 (1984) 941.
[16] J. Krupka, M. Klinger, M. Kuhn, A. Baranyak, M. Stiller, J. Hinken, J. Mmodelski, IEEE Trans. Appl. Supercond. 3 (1993) 3043.
[17] W.H. Chang, J. Appl. Phys. 50 (1979) 8129.
[18] M.R. Trunin, Phys.-Uspekhi. 41 (1998) 843.
[19] J.L. Tallon et al., Phys. Rev. Lett. 74 (1995) 1008.
[20] W.N. Hardy et al., Phys. Rev. Lett. 70 (1993) 3999.
[21] We note that in Ref. [1] due to the rough approximation used in extracting the magnetic penetration depth, $\Delta\lambda(T)$ for $\delta = 0.4$ was erroneously taken as quadratic temperature dependence. For example, we took the geometric factor $\Gamma = (1/2)\mu_0\omega d$ as a constant, but, in fact, it is a function of $\lambda(T)$. Here, we report a more accurate extraction method and take the temperature range to be $T < T_c/3$ to ensure a linear-T dependence for each δ value.

[22] D.A. Bonn, S. Kamal, K. Zhang, R. Liang, D.J. Baar, E. Klein, W.N. Hardy, Phys. Rev. B 50 (1994) 4051.
[23] D.J. Scalapino, Phys. Rep. 250 (1995) 329.
[24] P.A. Lee, X.-G. Wen, Phys. Rev. Lett. 78 (1997) 4111.
[25] X.-G. Wen, P.A. Lee, Phys. Rev. Lett. 80 (1998) 2193.
[26] M. Chiao, R.W. Hill, C. Lupien, L. Taillefer, P. Lambert, R. Gagnon, P. Fournier, Phys. Rev. B 62 (2000) 3554.
[27] A.C. Durst, P.A. Lee, Phys. Rev. B 62 (2000) 1270.
[28] M.J. Graf, S.-K. Yip, J.A. Sauls, D. Rainer, Phys. Rev. B 53 (1996) 15147.
[29] M. Sutherland et al., Phys. Rev. B 67 (2003) 174520.
[30] In Physica C 364–365 (2001) 408 we have reported a value of $\alpha^2 = 0.95$–1.07 for $\delta = 0.4$, which appeared to be in contradiction to our assertion of noting that α^2 is always smaller than 1. We note here that the discrepancy was mainly due to the limited available data on $\frac{v_F}{v_2}$ at that time. The experimental data reported by Sutherland et al. [29] showed that $\frac{v_F}{v_2}$ is strongly doping dependent and decreases with decreasing oxygen contents. With the correction made by using more accurate $\frac{v_F}{v_2}$ values at each δ, the values of α^2 are indeed all well below 1 and in better agreement with Lee and Wen's model.